Interactions of exhaled buoyant jet flow and human motion-induced airflow: an experiment study in a water tank

Fan Liu[a,b], Lei Zhang[a], Zhiwen Luo[c], Chongyang Zhang[d], Hua Qian[b,*]

[a] School of Environment and Architecture, University of Shanghai for Science and Technology, Shanghai, China

[b] School of Energy and Environment, Southeast University, Nanjing, China

[c] Welsh School of Architecture, Cardiff University, Cardiff, United Kingdom

[d] Shanghai Research Institute of Building Sciences (Group) Co., Ltd., Shanghai, China

*Corresponding author:

Hua Qian, Professor in Indoor Air Quality and Respiratory Infectious Disease Transmission

Postal address: School of Energy and Environment, Southeast University, 2 Sipailou, Nanjing, 210096, China

Email address: qianh@seu.edu.cn

Abstract: Indoor environments with displacement ventilation or under-floor air distribution commonly exhibit thermal stratification, which can impact the dispersion of droplets in exhaled air by moving human sources. This paper presented an experimental study using a water tank to simulate the coupling characteristics of exhaled airflow and human motion-induced oncoming airflow, especially in a stratified environment. The effects of exhalation velocity and movement speed were studied. Results show that the buoyant jet flow couples with the oncoming flow, firstly spreading forwards and upwards, forming the impinging region, where the penetration distance is found to vary linearly with the ratio of movement velocity and exhalation velocity. Then the coupled flow spreads backwards, forming the wake region behind the source, where the flow rises upwards, albeit at a slower rate than in motionless conditions. In the wake region, there is an obvious stagnant layer, which is exacerbated by the thermal

stratification of the ambient fluid and much lower than the lock-up height of motionless buoyant jet flow. It is expected to provide scientific basis for formulating prevention and control measures in public spaces.

Keywords: water tank experiment; expiratory airflow; moving source; thermal stratification; impinging region; stagnant layer

1. Introduction

During the COVID-19 pandemic, it has been found that the local accumulation of exhaled virus-laden droplets from the infected source in the crowded indoor space can easily cause cross-infection of SARS-CoV-2 [1]. States of the occupants are various in different-type buildings, such as rest in waiting halls, walking in exhibition gallery, and running in stadium, etc. Human activities can change the concentration distribution of aerosols and also cause a difference in the exhalation rate and virus emission rate [2-4]. These factors are important to determine the infection risk of susceptible people who share the indoor environment [5]. Investigations on the dynamic characteristics of the exhaled airflow and pollutant from infected patient in different motion states are of great significance for controlling disease transmission and making precautions, however less studied.

In different-type buildings like hospital, bus station, airport and sport hall, the ventilation strategy differs with special requirements for design, giving rise to various vertical temperature distributions in indoor environments [6]. For example, a vertical temperature difference of approx. 3 ℃ was observed in a classroom ventilated with displacement natural ventilation within 0.1 - 1.1 m at the location of students [7]. Zhao et al. [8] found in three arrival halls of an airport environment, the vertical temperature difference from 0 - 3 m was of about 6.5, 5.7 and 1.5 ℃, while only a small temperature difference of 0.2 ℃ in departure hall. A greater vertical temperature difference than the acceptable level in the occupied zone not only causes

the thermal discomfort, but may not be conducive to the diffusion and dilution of pollutants. The existing studies indicated that the vertical temperature difference of indoor air is mainly attributed to the heating, ventilation, and air-conditioning (HVAC) systems [9-12], air infiltration [10,11], occupant distribution [13], etc. In our recent work, the indoor air temperature data in different-type indoor environments in real world was retrieved from the published literature based on the measurements and compared [14]. Results show that the vertical temperature gradients in office building, hospital, classroom, etc. are within the range of -0.34 to 3.26 ℃/m. In large space such as coach station, airport terminal, and sport hall, the average temperature gradient ranges within 0.13-2.38 ℃/m in occupied zone (0-3m). Numerous studies have reported that for a motionless infected patient, the thermal stratification can make the exhaled airflow and airborne aerosols locked at a certain height [15-17], which increases the transmission distance of the virus-laden aerosols and exposure risk of susceptible people [5]. When people move in indoor space, wind flows over a human body, defined as the oncoming airflow [18], and interacts with the exhaled buoyant jet flow, as depicted in Fig.1. The coupled flow spreads driven by the reverse momentum and buoyance under the impact of thermal stratification of ambient air. However, how the thermal stratification affects the interaction of the coupled airflow and the exhaled aerosols remains unknown.

There have been extensive experimental measurements [19-23] and numerical simulations [21,24-27] on the impact of human motion on indoor airflow filed and pollutant distributions, but mostly with motionless pollutant source. In full-scale test rooms with manikins, Wu et al. [22] studied the impact of human moving on the dispersion of pollutant exhaled from a seated source, and found that human movement with a long time enhanced the mixing of the pollutant, but potentially increasing the human's exposure to exhaled aerosols. Similar conclusion was also given by early work of Wang and Chow [27], in which they found that increasing the speed of human walking can reduce the number concentration of suspended droplets. Liu et al. [23]

studied the effect of a circulating nurse walking on airflow and bacteria-carrying particles produced in the operating process, and found that as the circulating nurse passed, local concentration of the bioaerosols shed from surgical staff increased due to the airflow disturbance and resulted in an increased risk of surgical site infections. The above studies focused largely on the disturbance on the indoor airflow of the of human movement. They have well addressed the importance of human motion on airflow patterns and further caused aerosol suspension or secondary suspension, resulting a potential increase of exposure risk. In ventilated rooms, it has been identified that the existing of thermal stratifications of ambient air is an essential factor for the dispersion of aerosols, especially for the disease transmission via the exhaled virus [28-31]. In recently, Feng et al. [27] focused on the relationship between the thermal stratification in displacement ventilated room and human movement, and found that human movement can destroy of the stability of indoor air, and weaken the thermal stratification, while no further insights into how the exhaled buoyant jet flow and aerosols were affected in such stratified environment. Overall, much less is known about the dynamic characteristics of the exhaled airflow and aerosols from a moving infected source in indoor environments with a thermal stratification. The interaction mechanism of the exhaled buoyant jet flow and motion-induced airflow is the key basis for disease controlling in real-world settings.

Two experimental methods are widely used to understand the aerodynamic characteristics of indoor airflow and pollutant transmission, i.e., full-scale experiments [21-23,32,33] and reduced-scale experiments [19,20,30,34]. Full-scale experiments in ventilated chambers are often limited to several airflow patterns, in which the vertical temperature gradient is uncontrollable as needed. Water-tank modeling has gradually been proved to be an appropriate tool to simulate the airflow patterns in indoor environments due to its flexibility and convenience on boundary condition controls. For example, Luo et al. [19] studied the dynamic changes of the movement-induced wake flow in a thermally-uniform water tank using a 3D

printed scaled-down manikin. Mingotti et al. [34] explored the air mixing arisen from the human movement along a corridor using a cylinder in a thermally-uniform water wank. In the early work of Ghajar and Bang [35], they proposed a Modified Oster method to produce a stable density stratification in salt water, which was widely used in the experimental studies on urban heat island [36,37]. In our previous work [30], this method was developed by top heating and bottom cooling at the same time to establish stable temperature gradient of the ambient water in the tank. Two-way temperature control can reduce the time required to form a thermal stratification, and help maintain the stability. In addition, thermistors or thermochromic liquid crystals for temperature can be quite fast-response devices in water, which makes it possible for the measurement or visualization of the concentration and temperature distribution of the buoyant jet flow exhaled by human. However, experimental studies have been rarely carried out to observe the interactions between the exhaled buoyant jet flow and movement-induced airflow in thermally stratified environments.

In this study, reduced-scale experiments in water tank are used with two purposes: scaling the interaction of expiratory airflow and motion-induced airflow under feasible and controllable water-tank settings to explore the impact of thermal stratification on the dispersion of the coupled flow, and obtaining high-quality experimental data to validate the theoretical models or numerical simulations in our future work. The crucial issues related to disease transmission are expected be answered: what is the difference in the dynamic characteristics of the exhaled airflow between a motionless patient and a moving patient, and whether there is also a "lock-up" phenomenon when the exhaled buoyant jet flow couples with human motion-induced oncoming airflow in a thermally stratified environment. A scaled-down a cylinder being towed forwards is used to represent a moving person in the water tank with well controllable thermal environment. The exhaled airflow from the moving person is simulated by a buoyant jet flow. Interactions of the exhaled buoyant jet flow with different initial parameters and the motion-

induced airflow characterized by with different movement speeds are observed in the water tank. It is expected to clarify the synergistic effect of human respiratory activities and human motion on the exhaled flow dispersion, and furthermore contribute to predicting the contaminant transport process in public spaces.

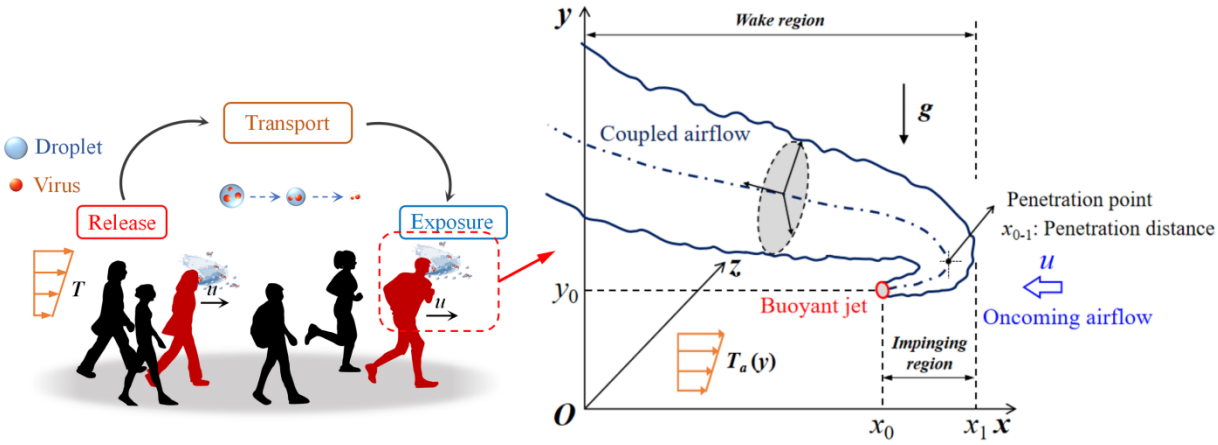

Fig. 1 Simplification of the coupled flow of exhaled buoyant jet flow and motion-induced oncoming airflow

2. Methodology

2.1 Similarity analysis

For a viscous, incompressible and stratified fluid, the governing equations of motion and thermodynamic energy are analogous in air and water systems. In this experiment, the water tank is used to simulate an indoor environment with or without temperature gradient. The human body is regard as a cylinder [20,38], mounted on a sliding block and towed by a motor, forming the oncoming flow. The human thermal plume is not considered here, like many experimental or numerical studies on the wake flow induced by human motion [20,39], according to findings of Wu et al. [40] and Oh et al. [41] that when a freestream velocity appears at approx. 0.2 m/s, the oncoming flow penetrates the thermal boundary layer leading to collapse of the rising plume and dominates the micro- airflow/environment near the human body. The respiratory air exhaled from the mouth or nostril is considered as a circular non-isothermal

buoyant jet flow [42,43]. The human mouth is scaled into a circular orifice, with the jet flow being discharged from a circular nozzle in the human body model. To simplify the complex breathing modes, the pulsating breathing mode of respiratory activities is simplified as constant velocity, which may overstate the airflow and particle dispersion, but meeting the actual needs of the evaluation of cross-infection risk for emergency response. Similarity requirements should be satisfied to mimic the flow dynamics of an expiratory jet flow exhaled from a moving human using a reduced-scale model in the tank.

2.1.1 Similarity requirements of the source movement

Dynamic similarities between the motion-induced airflow around the human body can be achieved by Reynolds number, *Re*. This method was frequently used in the experimental studies on the impact of human motion on indoor airflow field and pollutant distributions in water tank [19,20,34]. An adult with a waistline of approx. 85cm is scaled as a cylinder with a diameter of 4cm in the water tank experiment. The same Re is essential in the two systems:

$$Re=\frac{u_{\mathrm{g}}D_{\mathrm{b,g}}}{v_{\mathrm{g}}}=\frac{u_{\mathrm{w}}D_{\mathrm{b,w}}}{v_{\mathrm{w}}} \quad (1)$$

where u is the moving speed, D_{b} is the hydraulic diameter of human body, and v is the kinematic viscosity of the fluid. The subscript *g* stands for air (distinguished from the subscript *a* for indoor ambient air), and *w* for water. Therein the moving speed of the reduced-scaled model in the water tank can be attainable.

2.1.2 Similarity requirements of the exhaled buoyant jet flow

Non-dimensional forms of the governing equations of motion and thermodynamic energy in a stratified fluid are similar to those in Lu et al. [44]. For a jet flow, the dynamic similarity between laboratory experiments and real situations can be achieved by *Re*. A typical value of *Re* for an expiratory flow ranges from 2,500 to 12,500, with mouth diameter of 2cm and exhalation velocities of 2-10m/s. The *Re* attainable in the reduced-scale water tank model is about 2,000 to 8,000, with the opening size of 4 mm and initial velocities of 0.5-2 m/s, a little

small for a rigorous simulation. That means, the values of *Re* in the two systems are larger than the critical value that is required for fully turbulent flow, in which cases the jet flow becomes independent of *Re* [45]. Due to the temperature difference between the exhaled air and the ambient air, the jet flow rises upwards jointly driven by buoyancy force and inertia force. Therefore, the densimetric Froude number *Fr* becomes the governing criterion for describing the prototype flow, which must be duplicated in the water tank modeling:

$$Fr=\frac{u_{\mathrm{c,g}}}{\sqrt{g'_{\mathrm{c,g}}D_{\mathrm{m,g}}}}=\frac{u_{\mathrm{c,w}}}{\sqrt{g'_{\mathrm{c,w}}D_{\mathrm{m,g}}}} \tag{2}$$

where D_{m} is the diameter of the mouth opening, u_{c} is the axial velocity of jet flow (m/s) , $g_c^{'}=(\rho_a(z)-\rho_c)g/\rho_{ref}$ is the buoyant acceleration (m/s^2), ρ_c the axial density of jet flow (kg/m^3), $\rho_a(z)$ the ambient air density (kg/m^3) in the vertical direction *z* and ρ_{ref} a constant reference density (kg/m^3) with the Boussinesq approximation. Eq. (2) shows that when considering water as the ambient fluid for modeling in the experiment, it is necessary to define *Fr* in terms of density rather than temperature. Therefore, the initial velocity of the buoyant jet flow in a thermally uniform water tank is solved by Eq. (2), which is achieved by controlling the water pressure difference in the experiment.

When there is temperature gradient in the ambient fluid, the temperature variation in vertical direction causes a change in the fluid density, which makes the flow oscillate in the environment, i.e., buoyancy is the recovery force of the oscillation. The angular frequency at which a vertically displaced parcel will oscillate in the stratified environment can be described by buoyancy frequency $N=\sqrt{-\frac{g}{\rho_{ref}}\frac{d\rho_a}{dz}}$. At this point, the local *Fr* at the mouth opening can be approximated as:

$$Fr=\frac{u_{c,g}}{D_gN_g}=\frac{u_{c,w}}{D_wN_w} \tag{3}$$

2.2 Experimental setups and case description

2.2.1 Experimental setups

Experiments are performed in a transparent glass rectangular tank (Length × Width × Height = 2.4 m × 0.8 m × 0.8 m) filled with water at rest. The tank walls are made of 1.5-cm-thick glass to be transparent to the green laser sheet. The experimental apparatus includes stable jet flow system, thermal stratification system, underwater towed system and monitoring system, as illustrated in Fig. 2(a).

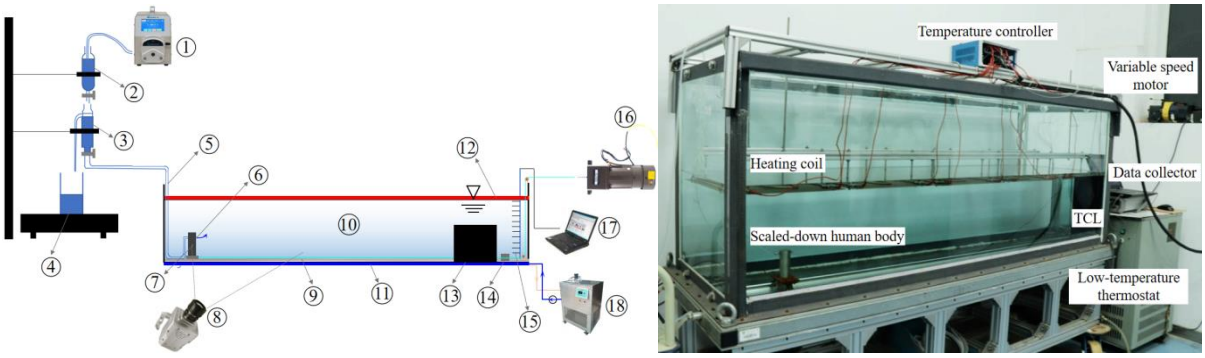

(a) (b)

Fig. 2 Schematic diagram of experimental system in (a) and photos of the setups in (b): ① Peristaltic pump; ② Liquid vessel; ③ Separator vessel; ④ Overflow collector; ⑤ Hose; ⑥ Nozzle; ⑦ Scaled-down human body; ⑧ Camera; ⑨ Slide rail; ⑩ Ambient fluid; ⑪ Cooling coil; ⑫ Heating coil; ⑬ TCL; ⑭ Spacing sliding block; ⑮ Thermocouple; ⑯ Variable speed motor; ⑰ Data collector; ⑱ Low-temperature thermostat

In all experiments, the heated liquid is first injected into separator vessel ③ until its level reaches the overflow surface. Then the upper valve is opened, and the heated liquid is then injected into liquid vessel ② to ensure a sustaining overflow status of ③ before opening the lower valve. A peristaltic pump (Kamoer Lab UIP WIFI-S183, China) ① is used here to continuously provide a stable supply. After these procedures, the lower valve is opened, then the liquid is injected into the ambient fluid through a circular nozzle ⑥ embedded in the cylinder ⑦, and a submerged horizontal round thermal jet is formed. The initial velocity of the buoyancy jet flow is controlled by the pressure difference between the liquid level in ③ and

the nozzle level. In indoor environments, the ratio of the mouth/nostril diameter (2cm) and room size (3-5m) is on the order of about 1:250-1:150. In this study, the corresponding ratio of the orifice size of the nozzle (4mm) and water-tank size (0.8 -2.4m) is on the order of about 1:600-1:200, so it can be considered that water tank is large enough for the injected flow to fully develop.

To simulate the forward movement of the source, the simplified body with the jet nozzle, together with the supply hose, is mounted on a sliding block on a slideway, which is towed by a motor ⑯ that is fixed outside the water tank. The sliding block is towed at a constant speed by the motor in the same direction of the discharging buoyant jet flow. The amplitude (i.e., the horizontal span of the movement) is 2m in all cases, for which a safety spacing sliding block ⑭ is fixed in the moving direction to stop the motion. In this work, for comparison purpose, a motionless buoyant jet flow is firstly observed in the water tank in each case; after the flow develops stably, the motor is started and a moving jet flow is formed, so the dispersion characteristics for motionless and moving buoyant jet flow can be clearly observed and compared.

The background water injected into the tank is regarded to be initially thermally uniform. To create a thermal stratification in the water, a U-type heating coil (10 kW) ⑫ on the upper surface of the water and a cooling coil ⑪ connected to a low-temperature thermostat (DC-1050, China) ⑱ via hoses and a small pump to form a circulation loop are arranged to realize a two-way temperature control to establish a stable temperature gradient in the tank. Fill water into the water tank until the U-type heating coil is just immersed by water surface. A temperature controller is fixed on the water tank to control the water temperature of the upper surface, i.e., after turning on ⑫, a targeted heating temperature is set and the real-time water temperature is displayed on the temperature controller. Heating starts when the set temperature is higher than the measured temperature; otherwise, heating stops. Similarly, a cooling

238 temperature is set on ⑱ and the cooling circulation starts to run when the water is lower than
239 the setting value. The temperature profile measurement of the water is conducted by 20
240 thermocouples ⑮, all calibrated and connected to a digital temperature logger (Agilent™
241 34970A), and a computer is used for data monitor and collect.

242 To track the trajectory of the moving buoyant jet flow, blue food dye is used and diluted
243 with a density close to that of the ambient fluid ⑩ to avoid the diffusion of mass transfer. The
244 temperature stratification can be visualized by the thermochromic liquid crystal (TLC) sheet
245 (Edmund Optics Inc., Barrington, NJ, USA) ⑬, the color of which changes from blue to red
246 as the temperature varies from the highest (25℃) to the lowest (20℃). A Canon camera ⑧ is
247 used to obtain the dispersion image and video of the moving buoyant jet flow, and fixed in front
248 of the water to ensure the consistency of all images photographed in different cases. Vertical
249 and horizontal coordinate scales are calibrated before the experiments on the left side and at the
250 bottom of the water tank to obtain the dispersion characteristics. The video records are analyzed
251 to provide the travelling distance and rising height of the coupled flow.

252 2.2.2 Case descriptions

253 Experiments are carried out to investigate the evolution of the coupled airflow of exhaled
254 airflow and oncoming airflow in both thermally-uniform and stratified indoor environments. In
255 the previous studies on the airflow disturbance induced by human motion, the moving speed
256 was generally set as >0.2m/s [19,23]. In our experiments, we focus on both the exhalation
257 airflow and the motion-induced airflow, so different ratios of the exhaled buoyant jet flow and
258 moving speed are included so that the results can be generalized to the dispersion of exhaled
259 pollutant from moving people with different respiratory activities. A low moving speed of
260 0.1m/s was set for the comparison with the mild exhalation like normal breathing with a low
261 velocity ratio; and higher moving speed was used for the comparison with the violent exhalation
262 like loudly speaking or coughing with a large velocity ratio. Therefore, we consider the impacts

of moving speed of the source person (Scenario 1: u_{moving}=0.1, 0.2 and 0.4m/s) and exhalation velocities (Scenario 2: $u_{exhalation}$=2, 5 and 10m/s) on the dispersion of the coupled flow in indoor environment. The modeling parameters in reduced-scale experiments are listed in Table 1, in which the u_{source} and u_{jet} represents the moving speed of the scaled-down human body and initial velocity of the buoyant jet flow, respectively. For comparison, both Scenarios 1 and 2 are conducted in the water tank with and without temperature gradient, so there is a total of 6×2=12 cases in two types of the water-tank environments. The dispersion behaviors of the coupled buoyant jet flow and the motion-induced oncoming flow such as the trajectory, development of the widths, and rising height can be obtained from processing of the captured tracer images for each experimental case. Before the experiments, the moving speed of the source is calibrated by changing the motor rotation speed in blank experiments where there is no buoyant jet flow emitted into the ambient water and only the source is towed forward in the water tank. In the experiments, each case is repeated three times to ensure that the visualized phenomena are consistent, and the standard deviation in the maximum rising heights is less than 10%.

Table 1 Experimental parameters in the model experiments

Scenario	u_{source} (m/s)	u_{jet} (m/s)	Ratio of u_{jet} and u_{source}	*Re*	*Fr*
1	0.05	2.20	44	1800	2130
	0.10	2.20	22	3600	2130
	0.15	2.20	15	7200	2130
2	0.05	0.45	9	1800	420
	0.05	1.10	22	1800	1060
	0.05	2.20	44	1800	2130

3. Results

3.1 Comparison of the buoyant jet flow discharged from motionless and moving source

The dispersal of buoyant jet flow discharged from the scaled-down source was visualized by the blue food dye. After repeating three times of each case, i.e., 3 conditions/case, we chose one condition of each case to show the experimental results. Here, the dispersion characteristics of the exhaled buoyant jet flow from a motionless source in both uniform and stratified environments are also included in our experiments for the comparison with the results from a moving source. As an illustrative example, the visualization images of the buoyant jet flow in thermally uniform water tank ($dT/dz=0$) when the source is motionless and moving with a speed of 0.05m/s are shown in Fig. 3(a) and (b), respectively. It can be found from Fig. 3(a) that the thermal flow disperses along the emitting direction and rise to the water surface quickly when the source is stationary, which has been frequently reported in many existing studies [16,17,35]. However, different phenomenon is observed of in Fig. 3(b) after the source moves forwards with a constant speed for 25s. The buoyant jet flow interacts with the airflow flow induced by the forward movement, forming the impinging region, as illustrated in Fig. 1. Under the effect of the oncoming flow, the forward momentum of the dyed fluid is dissipated, penetrating into the oncoming flow up to some axial direction, termed penetration point [46], where the horizontal momentum flux of the buoyant jet flow decays to zero. We defined the horizontal travelling distance from the nozzle to the and penetration point as the penetration distance. Then the coupled flow is turned backwards. The backwards thermal flow is affected by the buoyancy force and rises to the water surface, with instantaneous vortical structures during the dispersion, forming the wake region. As shown in Fig. 3(b), the horizontal travelling distance of the backward thermal flow is approx. $20D$ behind the source when it rises to the water surface, that is, the degree of upward bending of the thermal flow, is larger than that in Fig. 3(a) therein the forward spreading distance being only $6D$, which means the exhaled flow disperses for longer time in the wake region than that emitted by a motionless source.

Fig. 4 shows the dispersion characteristics of the coupled flow in a thermally stratified environment. For a buoyant jet flow from a motionless source, the temperature stratification of the ambient fluid will make it trapped at a certain height (i.e., *lock-up phenomenon*) along the human exhalation direction. In the experimental condition, as the photographic observation shown in Fig. 4(a), the buoyant jet flow goes from vertical to horizontal and becomes submerged due to the decreasing density with height; in addition, there are some oscillations before the buoyancy force and inertia forces reach equilibrium during the forward travelling process. This phenomenon has been clarified by experimental and theoretical studies [35,44], and the lock-up height was found to be a function of temperature gradient and initial parameters of the buoyancy jet flow when the source is motionless. When the source is moving forwards for 25s, as observed in Fig. 4(b), on reaching the penetration point and onwards, the backward flow also show a retention behind the source in the wake region, but significantly different from the lock-up phenomenon in Fig. 4(a). For comparison purpose, the lock-up layer of the motionless buoyant jet flow is denoted as *Zone 1* in Fig. 4(b), and the dispersion area of the coupled flow in the wake region is denoted as *Zone 2*. It can be clearly seen that *Zone 1* is in the height of > 6.5*D*, while *Zone 2* is much lower than *Zone 1* within a height of 3.5-5.5*D*, that is, when the oncoming flow interacts with the buoyant jet flow, there is a lower trapped layer of the coupled flow behind the moving source that is closer to the breathing zone of the susceptible people. When the source is moving forwards with a constant speed, an inverse sheared velocity induced by the oncoming flow leads to instabilities and cumulative entrainment in the wake region [47,48]. As a result, the coupled flow mixes quickly with the ambient fluid and the temperature decays more quickly to the water temperature, causing the buoyancy disappear at a low height and the flow stops rising and travels along this layer. In addition, faster attenuation of the momentum and temperature makes it easier for the inertia force and buoyancy force to reach equilibrium in the trapped layer, thus no obvious oscillations

in the wake region [30,49]. It implies that the human-motion-induced flow can facilitate the temperature and velocity decay of the exhalation airflow. However, when there is a thermal stratification in indoor environment, the pollutant is more easily trapped at the breathing zone behind the infected person. The susceptible people in the downstream from the source are more easily exposed to the airborne aerosols exhaled by the source compared to those who have a face-to-face exposure with the source.

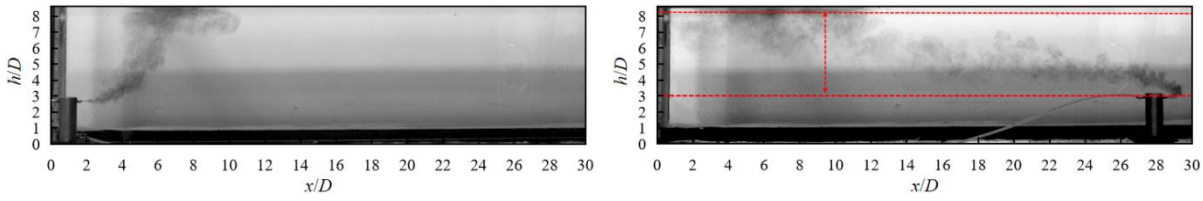

(a) (b)

Fig. 3 Visualizations of the thermal flow in thermally uniform water tank (u_{source}=0.05m/s, u_{jet}=2.20m/s, dT_{water}/dh=0): (a) from a motionless source; (b) from a moving source

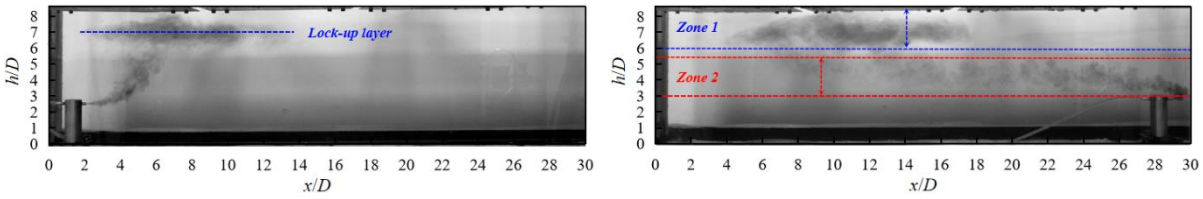

(a) (b)

Fig. 4 Visualizations of the thermal flow in thermally stratified water tank (u_{source}=0.05m/s, u_{jet}=2.20m/s, dT_{water}/dh=0.3℃/m): (a) from a motionless source; (b) from a moving source

3.2 Instantaneous evolution characteristics of coupled buoyant jet flow and oncoming flow

In Fig.5, we present a series of images at different times during the dispersion process of the coupled flow. The images were captured at times 5,15 and 25s after the beginning of each experiment. It can be found in Fig. 5(a) that at 5s there have been instantaneous large-scale vortical structures in the wake region, which originates from the instable shearing when the

oncoming flow is acting on the forward buoyant jet flow. After the source moves forwards for 10s, an approximately asymmetric development of these vortical structures can be found on the lower and upper sides of the flow. Due to the thermal stratification of ambient fluid, the decaying buoyancy force of the rising flow interacts with the increasing temperature, causing a clear stagnant layer in the wake region behind the source at 25s. These vortical flow structures is dissipated, evolved into small-scale turbulence and removed in the ambient fluid, which however takes some time to complete. In our results, after the source move forwards for 25s, the dye fluid behind the source can travels for about 20*D*, which implies that the source can carry the contaminants up to a long distance during the forward movement. Therefore, in the cases where people are moving indoors, keeping a distance of 1-2m may not be enough for the people behind the infected source. There is still a high possibility of being exposed directly to the virus-laden aerosols exhaled by the moving source person, such as queuing up in public station or slow walking in exhibition hall.

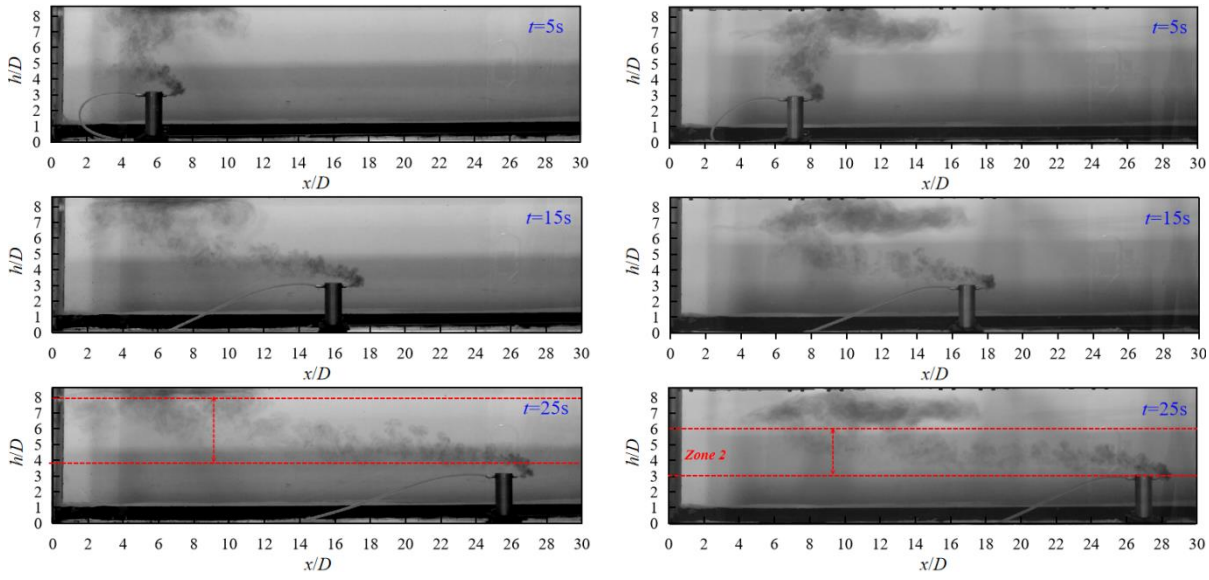

Fig. 5 Visualizations of the buoyant jet flow under Scenario 2:
(a) in thermally uniform environment; (b) in thermally stratified environment

3.3 Impact of motion speeds on evolution characteristics of the coupled flow

People move in a variety of ways in different-type indoor environments, such as walking slowly in exhibition gallery, walking fast and jogging in public stations and running in indoor stadium. To explore the impact of the moving speed of an infected person in different motion states on the dispersion of the exhaled airflow and containment dispersion, the scaled-down human body was towed with three different velocities, with *Re* increasing from 1800 to 7200, as the visualizations shown in Fig.6. It can be found from Fig. 6(a) that when the source is moving in a well-mixed environment with a small speed of 0.05m/s, the coupled flow can reach the water surface in the wake region. As the speed increases to 0.1m/s, the upward trend becomes unobvious and the concentration of the dyed fluid decays obviously; at the same time, the outlines begin to get thinner of 3*D*-6*D*. As the moving speed increases to 0.15m/s, there is no clear upward trajectory can be observed in the dispersion process, while a downward dispersion tend of the coupled flow appears behind the source, as reported in many existing studies [19,20,50]. It is mainly attributed to the entrainment of the coupled flow behind the moving source. The vortices of the wake flow could enhance the mixture of the discharged contaminant in the vertical direction and carry them into the track behind the body when the moving speed increases. It implies that there may exist an equilibrium between the buoyancy flux of the coupled flow and momentum flux of the motion-induced wake flow, i.e., a critical value of Re_c for the dispersion of the coupled flow in wake region, and when the $Re < Re_c$, the coupled flow is dominated by the buoyance and rises during the horizontal dispersion in the wake region; after reaching the Re_c, the coupled flow begins to spread downwards and behind the source due to the instabilities and cumulative entrainment of the motion-induced flow in the wake region. In a thermally stratified water tank, see Fig. 6(b), as the speed increases from 0.05m/s to 0.1m/s, the height of *Zone 2* becomes lower and the width of the coupled flow becomes smaller. The travelling height gets closer to people's breathing height as the moving speed increases. When *Re* is large enough to totally dominate the dispersion of the coupled flow,

the buoyant force disappears rapidly, and a similar downward dispersion of the dyed fluid can be seen behind the source. However, more experimental or numerical data are needed in our following work to find the value of Re_c in the environment with or without temperature gradient.

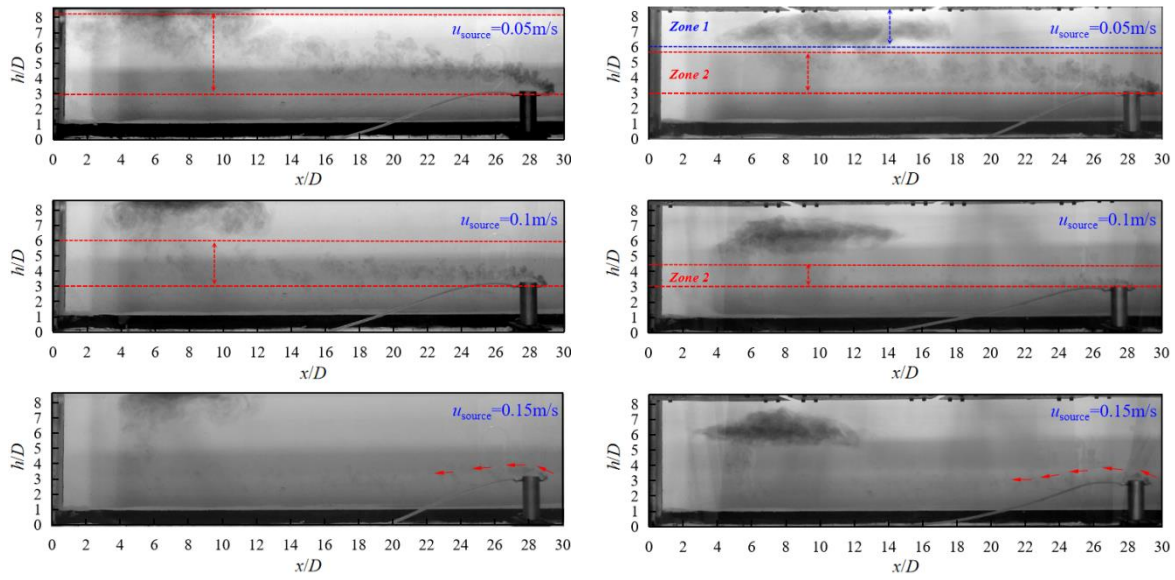

(a) (b)

Fig. 6 Visualizations of the buoyant jet flow under Scenario 1 (u_{jet}=2.2m/s): (a) in thermally uniform water; (b) in thermally stratified water

3.4 Impact of the buoyant jet velocity on evolution characteristics of the coupled flow

The intensity of the exhaled buoyant jet flow is determined by the respiratory activities of the infected source. Here, three initial velocities of the buoyant jet flow emitted by the moving source were compared in our experiments, with *Fr* increasing from 425 to 2126, as the results shown in Fig.7. A reverse relationship is found between the dispersion characteristic and *Fr* of the buoyant jet flow, compared to the results with increasing *Re* of the oncoming flow. With a small discharging velocity of 0.45m/s (*Fr*=425), the momentum flux and buoyancy flux for forward spreading are small, and the oncoming flow bent the coupled flow backwards with a small penetration distance. As *Fr* increases (with a velocity of 1.1m/s), the trajectory of the buoyant jet flow exhibits a significant rising within 3*D*-8*D* in the backward region in Fig. 7(a), while in stratified environment the thermal flow is still found to disperse at a low height layer.

As the coupled flow is turned backwards, the vertical rising continues due to the temperature difference. When the jet velocity increases to 2.2m/s (*Fr* increases to 2126), the dispersion trajectory becomes more obvious due to a high initial buoyancy flux and momentum flux of the coupled flow. The backward flow can rise to the water surface in uniform environment, while no obvious rising in stratified environment.

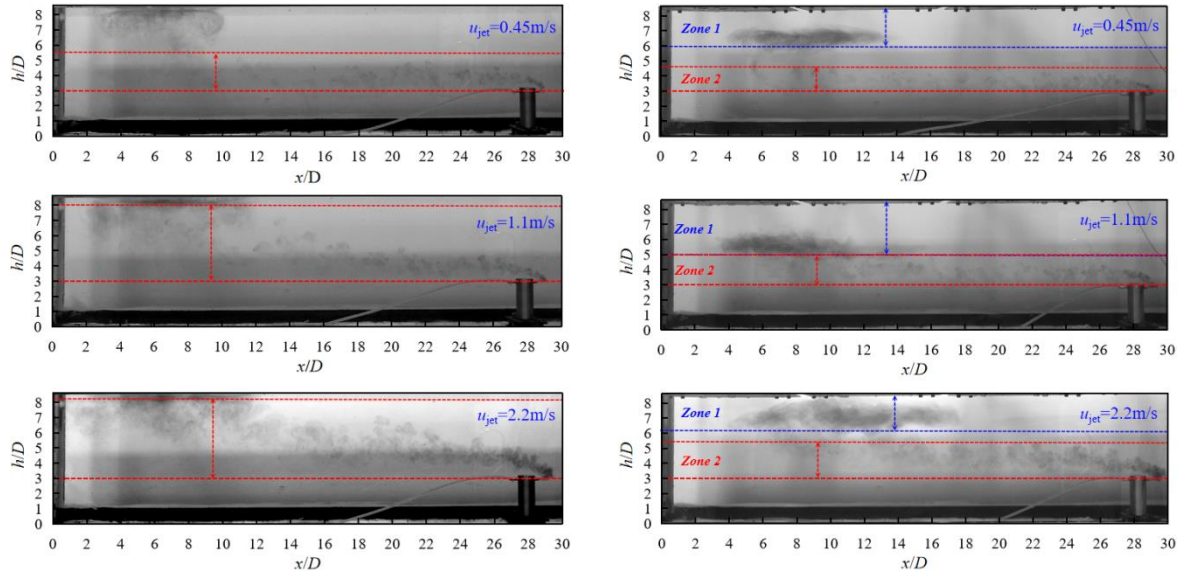

(a) (b)

Fig. 7 Visualizations of the buoyant jet flow under Scenario 2 (u_{source}=0.05m/s): (b) in thermally uniform water; (b) in thermally stratified water

4. Discussion

4.1 Synergistic impact of exhalation velocity and moving speed

Details of the experiments and the above results present that two regions are involved in the dispersion of the coupled flow, i.e., impinging region of the forward buoyant jet flow and the motion-induced oncoming flow, and the wake region of the coupled flow. Numerous studies were focused on the wake flow induced by human movement [19,24,38] or oncoming airflow [18,51], ignoring the buoyant jet flow exhaled from source and the interaction with the oncoming flow when people are moving. In the impinging region, the buoyant jet flow moves forwards and upwards due to the initial horizontal momentum and buoyancy. After reaching

the penetration point under the impact of the oncoming flow, the coupled flow is turned backwards into the wake region, and advected by the decaying buoyancy and the horizontal momentum of the oncoming flow. At a small movement speed (with a low *Re*), the initial momentum of the buoyant jet flow keeps it going forward for a long distance during which the jet rises through a vertical distance on reaching the penetration point. As the *Re* increases, the reverse shear of the oncoming flow dissipates the forward momentum rapidly, and the jet is bent backwards readily with little vertical rising, travelling along a lower height. This phenomenon is similar with the pollutant discharge characteristic in water environment with a counterflow, which was widely studied and provided a good basis for fluid coupling [46,52]. As the moving speed continues increasing, a downward dispersion occurs due to the strong entrainment of the wake flow behind human body, consistent with the findings of the work aimed only at the wake flow induced by fast motions indoors [19,20,50]. Zhao and Feng [53] compared the exhaled aerosol distribution field when source is walking in the leeward direction and windward direction of the ventilation airflow, and found that the background wind causes the aerosol to gather within a certain range behind the human body more easily. It has been identified that the entrainment rate for the increase of the flow mass is largely dependent on the centerline velocity [54], therefore, a large *Re* number increases the mixing rate with the ambient fluid, making the temperature difference disappears at a lower height (point A in Fig. 8(a)) where the backward flow stops rising and spreads along the *-x* direction, forming the stagnant layer. Similarly, as the *Fr* number becomes larger, the momentum flux, buoyancy flux and mass flux of the buoyant jet flow increase. After being discharged into the ambient fluid, the buoyancy force gradually disappears due to the increasing temperature of the ambient fluid with height in stratified environment, and finally causes the coupled flow travel along a lower horizontal layer close to the human's breathing height, as illustrated in Fig.8(b).

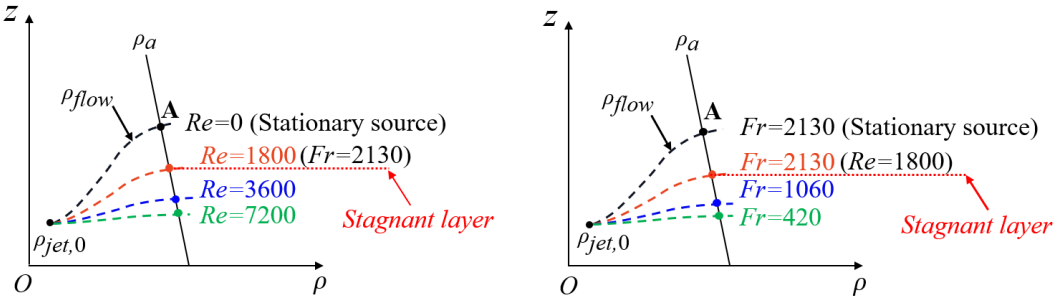

(a) (b)

Fig. 8 Density variation of the coupled flow in the dispersion with:

(a) increasing moving speed of the source; (b) increasing buoyant jet velocity

4.2 Quantitative relations in impinging region and wake region for assessment

The information on the interaction between the exhaled airflow and oncoming airflow is helpful in predicting airborne contaminant transport. Quantitative relations were further discussed for accessing the dispersion characteristics under the impact of exhalation velocity and moving speed. Considering the limited experimental cases in the present work, the penetration distance (l) of the coupled flow in impinging region and the rising height in the wake region, i.e., the maximum rising height of *Zone 2* (h) is fitted as relations varying with the ratio of the jet velocity u_{jet} and the movement speed u_{source} using the results of the experimental cases in Table 1, as shown in Fig. 9. It can be found from Fig. 9(a) that the forward penetration distance in the initial impinging region varies linearly with the velocity ratio, with the value of R^2=0.9057. A large velocity ration when the oncoming flow is relatively weak makes the coupled flow spread further. This finding is consistent with the early work by Lam and Chan [55], in which they focused on a jet flow penetrating a counterflow to describe the discharge of pollutants into the atmosphere or receiving waterbodies. In this work, to the best of the authors' knowledge, this is the first implementation of such fluid modeling to explore the dynamic characteristics of expiratory airflow and motion-induced airflow in indoor environments when thermal stratification exists. The finding in Fig. 9(a) suggests that the method is valid and the well-fitting linear relation can provide more details for the prediction

of the airflow or pollutant dispersion exhaled from a moving person in both thermally-uniform and stratified indoor environments. In Fig. 9(b), it can be observed that in the subsequent wake region, the rising height of the coupled flow in a thermally uniform environment is significantly higher than that in a stratified environment, which means that the flow spreads closer to the human respiratory zone when there is a thermal stratification in occupied zones. However, there is no significant fitting relation between the rising height and velocity ratio in Fig. (9). The identification of quantitative relation between the rising height, especially the stagnant layer height with the velocity ratio needs more experimental or simulated data in our following work.

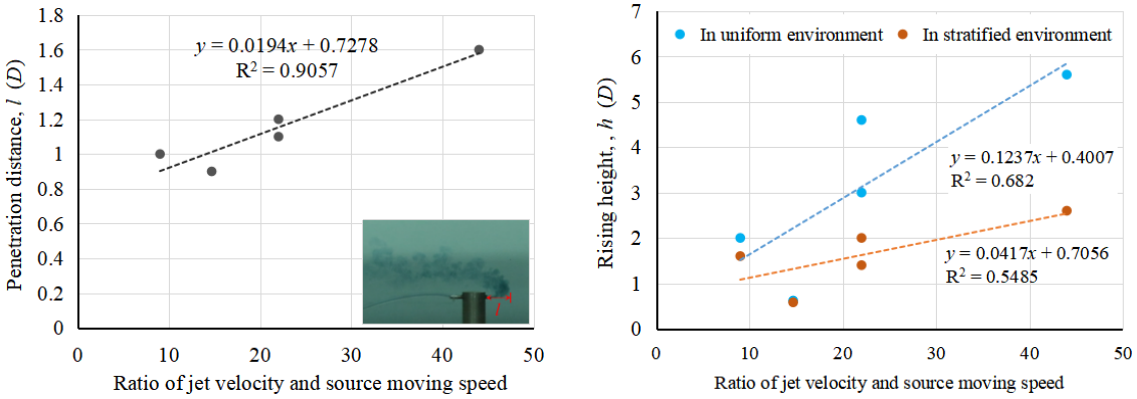

(a) (b)

Fig. 9 Relations of (a) penetration distance in the impinging region and (b) rising height in the wake region with different velocity ratios

4.3 Implications for infectious disease controlling in public spaces

The above findings imply that when the source person does vigorous exercise such as fast walking and running, the influence of the coupled buoyant jet flow and oncoming airflow on exhaled aerosols can last for >20s, and even for 30-60s as reported by Hang et al. [25]. In addition, the exhaled pollutant concentrated at a height close to the source's height in the downstream direction of motion, and travel a long horizontal distance, which is exacerbated by the positive thermal stratification of the ambient air. For both adults and children who follow the source, there is a significant risk of direct exposure to the aerosols exhaled by the source. For controlling disease spreading, safe social distance of 1-2m is implemented in many

497 countries [56,57], which is defined based on the droplet dynamics exhaled by a motionless
498 infected source [58,59], ignoring the various motion states of people in public spaces. Our
499 results, together with the earlier reports on the wake flow induced by human motion disturbance
500 shows that keeping a distance of 1-2m with the source may not be enough to avoid inhalation
501 risk; in addition, the following time of the susceptible people should also be controlled.
502 Furthermore, it has been reported that the expiratory rate and bioaerosol release rate of an
503 infected patient in motion are tens to hundreds of times of that in resting state [2,3,60-62], and
504 even show an exponential increase tend in high-intensity exercise state. In the recent work of
505 Buonanno et al. [4], they found that high emission rates of >100 quanta/h can be reached by an
506 asymptomatic subject who is walking slow and vocalizing, whereas the asymptomatic subject
507 in resting conditions mostly has a low quanta emission rate of <1 quantum/h. It further stressed
508 that the large emission of virus with high exhalation intensity from infected source in motion
509 states should be paid more attentions, rather than the motionless source.

510 **5. Conclusions**

511 Understanding the dispersion of the airflow exhaled from a moving infected patient plays
512 an important role in the transmission and controlling of respiratory diseases, especially in public
513 occasions with big population. In this work, the dynamics of the coupled flow of buoyant jet
514 flow exhaled from a source and the oncoming flow induced by the source motion in thermally
515 stratified environment was explored with reduced-scale experiments in a water tank. The
516 dispersion trajectories of the buoyant jet flow were compared when the source is stationary and
517 moving forwards, and the impact of initial velocity of buoyant jet flow and movement speed of
518 the source were investigated.

519 We found that different from a buoyant jet flow from a motionless source, there exist two
520 regions in the dispersion of the coupled flow when the source moves forwards, i.e., impinging
521 region and wake region. In the impinging region, the coupled flow rises upwards with a short

penetration distance, which is found to vary linearly with the velocity ratio of the jet velocity and movement speed. Then, the coupled flow spreads backwards and forms the wake region, where the flow disperses for a long time and over a long distance after the source. In the wake region, the coupled flow travels upwards, but more slowly than the rising speed when the source is motionless. It is noteworthy that when there exists a vertical temperature gradient of the ambient fluid, the coupled flow is easily trapped at a lower layer behind the source, which is found to be much lower than the "lock-up" height for a motionless buoyant jet flow and closer to the breathing zone of the people in the lee. A smaller moving speed and a larger jet velocity make the stagnant layer more obvious.

6. Limitations and prospects

There are some limitations for current study. The human body is simplified as a vertical cylinder, and there are no detailed walking gestures like bending of knees and elbows, which may cause the motion-induced wake flow behind human body different from the actual conditions. The pulsating breathing modes in realistic cases is simplified to be steady in the preliminary experiment, which may produce slightly modified results. Furthermore, only the flow interaction was studied in this experimental work, therefore the results are only valid for the situation when the exhaled droplets or droplet nuclei are smaller than 5-10μm that can follow the persons' exhalation flows. The transport behaviors of large droplets are different from those of small droplets and gaseous contaminants due to the relatively large gravity and drag force, which needs to be further studied in the future. In addition, in the experiments, it takes 3-4h to make a stable temperature stratification in the water tank for each experiment, so the number of the experimental cases was not large enough to make more quantitative analysis. We considered the present work as a preliminary study for our following studies, and the findings are mainly applicable to the early stage of design of an indoor environment.

In the following work, theoretical and numerical methods will be used to explore more detailed illustrations of the coupling mechanism of the exhaled buoyant jet flow and motion-induced oncoming airflow, and its further impact on the transmission of respiratory diseases.

Acknowledgement

This study was supported by Shanghai Sailing Program (No. 23YF1428700), Sixue Program of University of Shanghai for Science and Technology (No. 2022-SX-036) and the National Natural Science Foundation of China (No. 41977370).

References

[1] Qian H, Miao T, Liu L, Zheng X, Luo D, Li Y. Indoor transmission of SARS-CoV-2. *Indoor Air*. 2021;31:639-645.

[2] Cowie B, Wadlow I, Yule A, Janssens K, Ward J, Foulkes S, Humphries R, McGain F, Dhillon R, La Gerche A. Aerosol generation during high intensity exercise-implications for COVID-19 transmission. *Heart Lung and Circulation*. 2023;32:67-78.

[3] Zhang F, Shiue A, Fan Y, Liu J, Meng H, Zhang J, Leggett G. Dynamic emission rates of human activity in biological cleanrooms. *Building and Environment*. 2022;226:109777.

[4] Buonanno G, Stabile L, Morawska L. Estimation of airborne viral emission: Quanta emission rate of SARS-CoV-2 for infection risk assessment. *Environment International.* 2020;141:105794.

[5] Liu F, Luo Z, Li Y, Zheng X, Zhang C, Qian H. Revisiting physical distancing threshold in indoor environment using infection-risk-based modeling. *Environment International*. 2021;153:106542.

[6] Liu F, Luo Z, Qian H. Impact of thermal stratification on airborne transmission risk of SARS-CoV-2 in various indoor environments. *Building Simulation*. 2023.

[7] Wang Y, Zhao FY, Kuckelkorn J, Liu D, Liu J, Zhang JL. Classroom energy efficiency and air environment with displacement natural ventilation in a passive public school building. *Energy and Buildings*. 2014;70:258-270.

[8] Zhao K, Weng J, Ge J. On-site measured indoor thermal environment in large spaces of airports during winter. *Building and Environment*. 2020;167:106463.

[9] Espinosa FD, Glicksman LR. Determining thermal stratification in rooms with high supply momentum. *Building and Environment*. 2017;112:99-114.

[10]Liu X, Liu X, Zhang T. Theoretical model of buoyancy-driven air infiltration during heating/cooling seasons in large space buildings. *Building and Environment*. 2020;173: 106735.

[11]Liu X, Liu X, Zhang T. Influence of air-conditioning systems on buoyancy driven air infiltration in large space buildings: A case study of a railway station. *Energy and Buildings*. 2020;210:109781.

[12]. Zhao Y, Zhao K, Ge, J. Predicting the temperature distribution of a non-enclosed atrium and adjacent zones based on the Block model. *Building and Environment*. 2022;214:108952.

[13]Lan B, Yu ZJ, Huang G. Study on the impacts of occupant distribution on the thermal environment of tall and large public spaces. *Building and Environment*. 2022;218:109134.

[14]Liu F, Luo Z, Qian H. Impact of thermal stratification on airborne transmission risk of SARS-CoV-2 in various indoor environments. *Building Simulation*, 2023;16:1159-1172.

[15]Zhou Q, Qian H, Ren H, Li Y, Nielsen PV. The lock-up phenomena of exhaled flow in a stable thermally-stratified indoor environment. *Building and Environment*. 2017;116:246-256.

[16]Qian H, Li Y, Nielsen PV, Hyldgaard CE, Wong TW, Chwang AT. Dispersion of exhaled droplet nuclei in a two-bed hospital ward with three different ventilation systems. *Indoor Air*. 2006;16:111-128.

[17]Liu F, Zhang C, Qian H, Zheng X, Nielsen PV. Direct or indirect exposure of exhaled contaminants in stratified environments using an integral model of an expiratory jet. *Indoor Air*. 2019;29:591-603.

[18]Inthavong K, Ge QJ, Li XD, Tu JY. Detailed predictions of particle aspiration affected by respiratory inhalation and airflow. *Atmospheric Environment*. 2012;62:107-117.

[19]Luo N, Weng W, Xu X, Fu M. Experimental and numerical investigation of the wake flow of a human-shaped manikin: Experiments by PIV and simulations by CFD. *Building Simulation*. 2018;11:1189-1205.

[20]Gunasekera S, Li X, Lester D, Rosengarten G. Towards understanding the influence of human movement on aerosol dispersion. 23rd Australasian Fluid Mechanics Conference-23AFMC, Sydney, Australia, 4-8 December 2022.

[21]Han ZY, Weng WG, Huang QY. Numerical and experimental investigation on the dynamic airflow of human movement in a full-scale cabin. *HVAC&R Research*. 2014;20:444-457.

[22]Wu J, Weng W, Fu M, Li Y, Lan M. Enhancement effect of human movement on the high risk range of viral aerosols exhaled by a sitting person. *Building and Environment*. 2022;218:109136.

[23]Liu Z, Liu H, Rong R, Cao G. Effect of a circulating nurse walking on airflow and bacteria-carrying particles in the operating room: An experimental and numerical study. *Building and Environment*. 2020;186:107315.

[24]Tao Y, Inthavong K, Petersen P, Mohanarangam K, Yang W, Tu J. Vortex structures and wake flow analysis from moving manikin models. *Indoor and Built Environment*. 2021;30:347-362.

[25]Hang J, Li Y, Jin R. The influence of human walking on the flow and airborne transmission in a six-bed isolation room: Tracer gas simulation. *Building and Environment*. 2014;77:119-134.

[26]Feng L, Zeng F, Li R, Ju R, Gao N. Influence of manikin movement on temperature stratification in a displacement ventilated room. *Energy and Buildings*. 2021;234:110700.

[27]Wang J, Chow TT. Numerical investigation of influence of human walking on dispersion and deposition of expiratory droplets in airborne infection isolation room. *Building and Environment*. 2011;46:1993-2002.

[28]Bjørn E, Nielsen PV. Dispersal of exhaled air and personal exposure in displacement ventilated rooms. *Indoor air*. 2002;12:147-164.

[29]Gao N, He Q, Niu J. Numerical study of the lock-up phenomenon of human exhaled droplets under a displacement ventilated room. *Building Simulation*. 2012;5:51-60.

[30]Liu F, Qian H, Luo Z, Wang S, Zheng X. A laboratory study of the expiratory airflow and particle dispersion in the stratified indoor environment. *Building and Environment*. 2020;180:106988.

[31]Nielsen PV, Xu C. Multiple airflow patterns in human microenvironment and the influence on short-distance airborne cross-infection-A review. *Indoor and Built Environment*. 2022;31:1161-1175.

[32]Han M, Ooka R, Kikumoto H, Oh W, Bu Y, Hu S. Measurements of exhaled airflow velocity through human coughs using particle image velocimetry. *Building and Environment*. 2021;202:108020.

[33]Ren J, He J, Guo L, Li H, Kong X. Effect of walking modes and temperatures on the robustness of ventilation systems in the control of walking-induced disturbances. *Aerosol and Air Quality Research*. 2022;22:220115.

[34]Mingotti N, Wood R, Noakes C, Woods AW. The mixing of airborne contaminants by the repeated passage of people along a corridor. *Journal of Fluid Mechanics*. 2020;903:A52.

[35]Ghajar AJ, Bang K. Experimental and analytical studies of different methods for producing stratified flows. *Energy*. 1993;18:323-334.

643 [36]Fan Y, Y. Li, X. Wang, Catalano F. A new convective velocity scale for studying diurnal
644 urban heat island circulation. *Journal of Applied Meteorology and Climatology*. 2016;55:2151-
645 2164.
646 [37]Fan Y, Li Y, Yin S. Interaction of multiple urban heat island circulations under idealized
647 settings. *Building and Environment*. 2018;134:10-20.
648 [38]Tao Y, Inthavong K, Tu J. A numerical investigation of wind environment around a
649 walking human body. *Journal of Wind Engineering and Industrial Aerodynamics*. 2017;168:9-
650 19.
651 [39]Tao Y, Inthavong K, Petersen P, Mohanarangam K, Yang W, Tu J. Vortex structures and
652 wake flow analysis from moving manikin models. *Indoor and Built Environment.* 2021; 30(3):
653 347-362.
654 [40]Wu Y, Gao NP. The dynamics of the body motioninduced wake flow and its effects on the
655 contaminantdispersion. *Building and Environment*. 2014; 82:63-74.
656 [41]Oh W, Kato S. The effect of airspeed and wind direction on human's thermal conditions
657 and air distributionaround the body. *Building and Environment*. 2018;141:103-116.
658 [42]Chen W, Zhang N, Wei J, Yen HL, Li Y. Short-range airborne route dominates exposure
659 of respiratory infection during close contact. *Building and Environment*. 2020;176:106859.
660 [43]Liu F, Qian H, Luo Z, Zheng X. The impact of indoor thermal stratification on the
661 dispersion of human speech droplets. *Indoor Air*. 2021;31:369-382.
662 [44]Lu J, Arya SP, Snyder WH, Jr REL. A laboratory study of the urban heat island in a calm
663 and stably stratified environment. Part II: velocity field. *Journal of Applied Meteorology*.
664 1997;36:1392-1402.
665 [45]Townsend AA. The structure of turbulent shear flow. Cambridge Univ. Press, Cambridge,
666 England. 1956;315.

667 [46]Lam KM, Lee WY, Chan CH, et al. Global behaviors of a round buoyant jet in a
668 counterflow. *Journal of Hydraulic Engineering*. 2006;132(6):589-604.
669 [47]Lee JHW, Cheung V. Generalized lagrangian model for buoyant jets in current. *Journal of*
670 *Environmental Engineering*. 1990;116:1085-1106.
671 [48]Jirka GH. Integral model for turbulent buoyant jets in unbounded stratified flows. Part I:
672 Single round jet. *Environmental Fluid Mechanics*. 2004;4:1-56.
673 [49]Lee JHW, Chu VH. Turbulent jets and plumes: A lagrangian approach, Kluwer Academic,
674 Boston. 2003.
675 [50]Wu Y, Gao N. The dynamics of the body motion induced wake flow and its effects on the
676 contaminant dispersion. *Building and Environment*. 2014;82:63-74.
677 [51]Li C, Ito K. Numerical and experimental estimation of convective heat transfer coefficient
678 of human body under strong forced convective flow. *Journal of Wind Engineering and*
679 *Industrial Aerodynamics*. 2014;126:107-117.
680 [52]Lam KM, Chan C. Time-averaged mixing behavior of circular jet in counterflow: Velocity
681 and concentration measurements. *Journal of Hydraulic Engineering*. 2002;128(9):861-865.
682 [53]Zhao Y, Feng Y. Aerosol transmission risk of COVID-19 when passengers move slowly in
683 a line at the airport terminal. *E3S Web of Conferences*. 2022;356:05023.
684 [54]Turner JS. Turbulent entrainment-The development of the entrainment assumption, and its
685 application to geophysical flows. *Journal of Fluid Mechanics*.1986:173:431-471.
686 [55]Lam KM , Chan HC. Round jet in ambient counterflowing stream. *Journal of Hydraulic*
687 *Engineering*. 1997;123(10):895-903.
688 [56]Jones NR, Qureshi ZU, Temple RJ, Larwood JPJ, Greenhalgh T, Bourouiba L. Two metres
689 or one: What is the evidence for physical distancing in covid-19? *The BMJ*. 2020;370:m3223.

690 [57]WHO. Coronavirus disease (COVID-19) advice for the public
691 (https://www.who.int/emergencies/diseases/novel-coronavirus-2019/advice-for-public).
692 World Health Organisation. 2023.
693 [58]Wells WF. On airborne infections: study II. Droplets and droplet nuclei. *American Journal*
694 *of Epidemiology*. 1934;20:611-618.
695 [59]Liu L, Li Y, Nielsen PV, Wei J, Jensen RL. Short-range airborne transmission of expiratory
696 droplets between two people. *Indoor Air*. 2017;27:452-462.
697 [60]Mutsch B, Heiber M, Grätz F, Hain R, Schönfelder M, Kaps S, Schranner D, Kähler CJ,
698 Wackerhage H. Aerosol particle emission increases exponentially above moderate exercise
699 intensity resulting in superemission during maximal exercise. *Proceedings of the National*
700 *Academy of Sciences of the United States of America*. 2022;19:e2202521119.
701 [61]Orton CM, Symons HE, Moseley B, Archer J, Watson NA, Philip KEJ, Sheikh S, Saccente-
702 Kennedy B, Costello D, Browne WJ, Calder JD, Bzdek BR, Hull JH, Reid JP, Shah PL. A
703 comparison of respiratory particle emission rates at rest and while speaking or exercising.
704 *Communications Medicine (Lond)*. 2022;2:44.
705 [62]Wilson NM, Marks GB, Eckhardt A, Clarke A, Young F, Garden FL, Stewart W, Cook
706 TM, Tovey ER. The effect of respiratory activity, ventilatory therapy and facemasks on total
707 aerosol emissions. *medRxiv*. 2021; 02.07.21251309.
708
709
710
711